Performance Analysis of Intelligent Reflecting Surface-Aided Mobile Edge Computing Network with Uplink NOMA Scheme

Dac-Binh Ha[1,2(✉)], Van-Truong Truong[1,2], and Van Nhan Vo[2,3]

[1] Faculty of Electrical-Electronic Engineering, School of Engineering and Technology, Duy Tan University, Da Nang 550000, Vietnam
hadacbinh@duytan.edu.vn, truongvantruong@dtu.edu.vn
[2] Institute of Research and Development, Duy Tan University, Da Nang 550000, Vietnam
vonhanvan@dtu.edu.vn
[3] Faculty of Information Technology, School of Computer Science, Duy Tan University, Da Nang 550000, Vietnam

Abstract. This paper investigates the system performance of an intelligent reflecting surface-assisted mobile edge computing (MEC) network under Nakagami-m fading channel with an uplink non-orthogonal multiple access (NOMA) scenarios. The considered system consists of an access point (AP), two NOMA users, i.e., a cell-center user and a cell-edge user, and a two-dimensional passive element array of the intelligent reflecting surface (IRS). Specifically, we consider the IRS to act as a relay to help cell-edge users offload tasks to the AP. We derive closed-form expressions of the successful computation probability (SCP) to evaluate the system performance. Furthermore, we analyze the ceiling SCP when the system operates in the high-SNR regime to clarify the system further. Finally, we investigate the impact of critical system parameters on the behavior of this considered system to look insight into the performance. The simulation results confirm the accuracy of our analysis.

Keywords: Intelligent reflecting surface · Mobile edge computing · MEC server · Non-orthogonal multiple access · Successful computation probability · Uplink NOMA

1 Introduction

Many sensor nodes (SN) and machines were connected via wireless links in the Fourth Industrial Revolution era. However, since these nodes typically have limited computing capabilities, they cannot complete tasks that require large amounts of computation in instantaneous time, not responding in real-time [1]. In order to address this issue, servers with small-scale data centers, which usually are co-located with the access points (APs) or base station (BS), can be deployed

N.-S. Vo et al. (Eds.): INISCOM 2022, LNICST 444, pp. 48–61, 2022.
https://doi.org/10.1007/978-3-031-08878-0_4

at the edge of the network, delivering compute resources that help mobile devices complete a task. Therefore, these resource-intensive nodes can offload their tasks to APs for computing and obtain the results in real-time requirements via wireless links. This approach is mentioned as mobile edge computing (MEC) [2].

In addition, the non-orthogonal multiple access (NOMA) technique has been proposed to be integrated into MEC systems to increase the number of connections, and enhance spectrum efficiency and energy efficiency [3–6]. Zhow *et al.* in [3] investigates the NOMA MEC system and the problem of optimizing computational performance in two schemes, i.e., partial offloading and local computation. Meanwhile, the work [6] investigate the NOMA-MEC model in the wireless sensor network (WSN). The results show that the NOMA-MEC network performance is significantly superior to the traditional OMA method. However, NOMA MEC models still have many problems to be studied [7,8], such as user pairing issues or resource allocation issues. For instance, the more significant the difference in channel gain of the cell-center user and the cell-edge user, the higher the overall sum capacity, but the cell-edge user may encounter a risk of achieving a meager offloading success rate, reducing the overall performance of the system.

Therefore, integrating relaying and cooperative communication schemes into the NOMA-MEC network can help improve cell-edge user performance [9–12]. Indeed, relay-aided transmission models have been indicated to increase transmission reliability, network coverage, and achievable rate. Specifically, the authors in [12] presented promising NOMA-MEC-based relaying architectures and analyzed their advantages for both uplink and downlink. However, [13] stated that the drawbacks in current network technology are that it can only handle the transmitter and receiver, not the environment in between.

Recently, intelligent reflecting surfaces (IRS), which consist of a two dimensional passive element array, has been proposed as an effective solution to enhance the performance of next-generation wireless communication networks [14–16]. Each element of IRS can independently incur some change to the incident signal, e.g., the phase, amplitude, frequency, or even polarization. Therefore, an IRS intelligently configures the wireless environment to aid the transmissions between the base station and far users when direct links have low qualities. There have been several studies on independently integrating IRS with MEC [17,18], and IRS with NOMA [19–21], to maximize the advantages of these techniques.

Obviously, the integration of IRS into NOMA-MEC systems opens up a potential research direction, contributing to realizing the future MEC network [22–24]. Zhou *et al.* propose a two-user IRS-NOMA-MEC model with a novel NOMA time-sharing scheme that allows the system to switch using NOMA or TDMA. The authors investigate the system with two scenarios where the computing power of the MEC server is finite and infinite. Wang *et al.* studied a massive users NOMA-MEC IoT model with the help of multiple reflecting elements IRS. The authors state the problem of maximizing energy efficiency and propose a semidefinite programming relaxation algorithm to solve this non-convex problem. In the work [25], Li *et al.* consider an IRS wireless-powered NOMA MEC IoT network. Specifically, IoT devices (IDs) can harvest energy from a power

station directly and through a reflected channel via IRS. The ID then uses the collected energy to offload the task to the AP using the uplink NOMA protocol. Simulation results clarified the effect of the IRS on the system in the absence of its use.

Motivated by [21], this paper considers an IRS-aided NOMA MEC network in which a cell-center user and an IRS-aided cell-edge user intend to offload their tasks to a MEC AP. The main contributions of our work are as follows:

- We investigate a MEC system model and IRS-NOMA protocol for this system.
- We derive the closed-form expressions for the successful computation probability (SCP) and ceiling in the high-SNR regime.
- To look insight into the behavior of this system, we investigate the impact of critical system parameters on the system performance.

The other parts of our paper is organized as follows. The system model of MEC based on IRS-NOMA protocol is described in Sect. 2. In Sect. 3, SCP is analyzed, closed-form expression is obtained. The numerical results and discussion are provided in Sect. 4. Finally, the conclusions and future works are presented in Sect. 5.

2 System Model

Let us consider an IRS-aided mobile edge computing NOMA network as shown in Fig. 1. In which, two resource-constrained mobile devices (MD), i.e., U_1 and U_2, offload their computation-intensive tasks to MEC with the support of IRS. More specifically, U_1 is the near user, i.e., the cell-center user, which can offload its tasks to AP directly. While U_2 is the far user, i.e., the cell-edge user, which needs assistance from the IRS for offloading because there is no direct channel from U_2 to AP due to large distances or/and blocking objects. The edge computing server, specifically the MEC server, is located at the AP. Suppose these two devices are connected by high data-rate optical fiber [17]. The IRS consisted of N passive reflecting elements placed in the cell to assist the users' computation offloading. Assumed that the element spacing of the IRS is large enough so that the small-scale fading associated with two different, reflecting elements is independent. We assumed that all devices are equipped with a single antenna and operate in the half-duplex mode under Nakagami-m fading.

Our proposed model is especially suitable for intelligent communication systems in IoT applications or smart factories [26,27]. For instance, SNs or machines in IoT systems will have difficulty communicating with APs in urban environments due to obstructions. However, the IRS deployed on the buildings will solve this problem by supporting the communication by creating a possible connection between both ends.

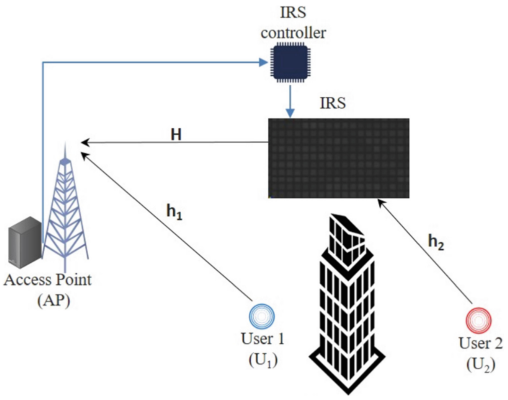

Fig. 1. System model

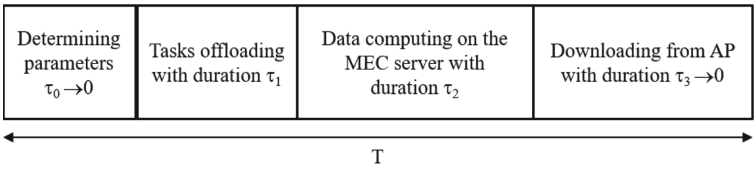

Fig. 2. Time flow chart for uplink IRS-aided NOMA MEC network

Assumed that U_1 and and U_2 have L_1 and L_2 bit tasks, respectively, that need to be processed. However, these tasks cannot be processed locally within the maximum allowable delay due to the computational limitations of MDs. Therefore, U_1 and U_2 offload their tasks to the AP, and the MEC server will assist in the processing. The channel state information (CSI) of all channels in proposed system is assumed perfectly known at MEC AP [6,28,29]. Note that the AP-U_1 link is assumed to be NLoS, while the links of AP-IRS and IRS-U_2 can be either LoS or NLoS for different scenarios. The small-scale fading vectors of the links of AP-IRS, AP-U_1 and U_2-IRS denoted by $\mathbf{H} \in \mathbb{C}^{1\times N}$, $\mathbf{h_1} \in \mathbb{C}^{1\times 1}$ and $\mathbf{h_2} \in \mathbb{C}^{N\times 1}$, respectively. More specifically, they are $\mathbf{H} = [h_{01}, h_{02}, ..., h_{0N}]$, $\mathbf{h_1} = [h_{11}]$ and $\mathbf{h_2} = [h_{21}, h_{22}, ..., h_{2N}]^T$, respectively.

We continued to propose an offloading protocol, called the IRS-NOMA scheme, for the MEC network, as shown in Fig. 2.

- In the first phase, namely the parameter determining phase, the MDs U_1 and U_2 estimate the CSI at the beginning of each communication in period τ_0.
- In the second phase, namely the offloading phase, U_1 and U_2 are paired together and apply the uplink NOMA technique to offload their tasks to the MEC server during period τ_1. Based on the principle of NOMA, the received signal of offloading tasks at AP is expressed as:

$$y = \mathbf{h_1}\sqrt{\frac{\rho P_U}{{d_1}^{\alpha_1}}}s_1 + \mathbf{H\Phi h_2}\sqrt{\frac{(1-\rho)P_U}{{d_{21}}^{\alpha_2}{d_{22}}^{\alpha_2}}}s_2 + n, \tag{1}$$

where P_U denotes the total transmit power of MD; ρ represents the power allocation ratio; s_i denotes for the offloading task of the i^{th} user, $i \in \{1, 2\}$; d_1, d_{21} and d_{22} denote the horizontal distances from AP to U_1, from AP to IRS and from IRS to U_2, respectively; α_1 stands for the path loss exponent of the link from AP to U_1; α_2 represents the path loss exponent of the link from AP to IRS and from U_2 to IRS; $n \sim \mathcal{CN}(0, \sigma^2)$ denotes the additive white Gaussian noise (AWGN) at AP; $\mathbf{\Phi} \triangleq \text{diag}\left[\beta_1 e^{j\theta_1}, \beta_2 e^{j\theta_2}, ..., \beta_N e^{j\theta_N}\right]$, $j = \sqrt{-1}$, is a diagonal matrix with $\beta_n \in [0, 1]$ is the amplitude-reflection and $\theta_n \in [0, 2\pi)$ is the phase-shift variable of the n^{th} element of IRS.

– In the third phase, namely the computing phase, according to the uplink NOMA concept, AP first decodes the signal of U_1 by treating the signal from U_2 as interference and then subtracts s_1 from y to obtain s_2. Hence, the signal-to-interference-plus-noise ratio (SINR) and the signal-to-noise ratio (SNR) at AP to decode s_i are respectively written as

$$\gamma_{U_1} = \frac{\rho\gamma_U\eta|h_{11}|^2}{(1-\rho)\gamma_U\mu|\mathbf{H\Phi h_2}|^2 + 1} = \frac{\rho\gamma_U\eta X}{(1-\rho)\gamma_U\mu Y + 1}, \tag{2}$$

$$\gamma_{U_2} = (1-\rho)\gamma_U\mu|\mathbf{H\Phi h_2}|^2 = (1-\rho)\gamma_U\mu Y, \tag{3}$$

where $\gamma_U \triangleq \frac{P_U}{\sigma^2}$ is the transmit SNR of users, $\eta \triangleq {d_1}^{-\alpha_1}$, $\mu \triangleq (d_{21}d_{22})^{-\alpha_2}$, $X \triangleq |h_{11}|^2$, $Y \triangleq |\mathbf{H\Phi h_2}|^2$. In this phase, these tasks are accomplished on the MEC server in period τ_2.

– Finally, in the last phase, namely the result returning phase, AP returns the computation results to users during period τ_3.

The time flow chart for the uplink IRS-aided NOMA MEC network is as Fig. 2, in which τ_0, as well as τ_3 are assumed very small compared to transmission time and thus are ignored [3,29].

Note that h_{0n}, h_{11} and h_{2n}, $n \in \{1, 2, .., N\}$, follow the Nakagami-m fading model with fading parameters, m_H, m_{h1} and m_{h2}, respectively, i.e., the probability density function of them is given by

$$f(x) = \frac{2m^m x^{2m-1}}{\Gamma(m)}e^{-mx^2}, \tag{4}$$

where $\Gamma(.)$ is the gamma function, $m \in \{m_H, m_{h1}, m_{h2}\}$. Note that the NLoS condition is achieved when $m = 1$ is set, while the LoS condition is attained when $m > 1$ [30].

3 Performance Analysis

This section presents the performance analysis based on the criterion of successful computation probability (SCP). The SCP, denoted by Ω_s, is used as a vital

metric to describe the performance of a MEC system [6,28,29]. By definition, Ω_s is the probability that all tasks are successfully offloaded, computed, and feedbacked to the MDs within the maximum allowable system delay $T > 0$, which is expressed as

$$\Omega_s = \Pr\left(\tau_1 + \tau_2 \leq T\right), \tag{5}$$

where

$$\tau_1 = \max\left\{\frac{L_1}{B\log_2(1+\gamma_{U_1})}, \frac{L_2}{B\log_2(1+\gamma_{U_2})}\right\}, \tag{6}$$

in which B denotes the channel bandwidth.

$$\tau_2 = \frac{\xi(L_1+L_2)}{f}, \tag{7}$$

where ξ and f denote the number of CPU cycles needed for executing each bit and the CPU-cycle frequency of the MEC server, respectively.

Similar to [21], we adjust the parameters of the IRS to obtain the best channel quality for U_2, i.e., to maximize $|\mathbf{H\Phi h_2}|$. Note that,

$$|\mathbf{H\Phi h_2}| = |\sum_{n=1}^{N} \beta_n h_{0n} h_{2n} e^{j\theta_n}|, \tag{8}$$

thus, the phase-shift variables of all $h_{0n}h_{2n}e^{j\theta_n}$ are set to be the same, e.g., $\theta_n = \theta^* - \arg(h_{0n}h_{2n})$, where θ^* is an arbitrary constant, $\theta^* \in [0, 2\pi)$. For simplicity, we assume that $\beta_n = 1, \forall n$. Therefore, after deploying the optimal phases θ_n, we have

$$Y = |\mathbf{H\Phi h_2}|^2 = \left(\sum_{n=1}^{N} |h_{0n}||h_{2n}|\right)^2 \tag{9}$$

According to [21], we implement the cummulative density function (CDF) and probability function (PDF) of the random variable Y as follows:

$$F_Y(x) = e^{-\frac{\lambda}{2}} \sum_{i=0}^{\infty} \frac{\lambda^i \gamma\left(i+\frac{1}{2}, \frac{x}{2N(1-\nu)}\right)}{i! 2^i \Gamma\left(i+\frac{1}{2}\right)}, \tag{10}$$

$$f_Y(x) = e^{-\frac{x}{2N(1-\nu)} - \frac{\lambda}{2}} \sum_{i=0}^{\infty} \frac{\lambda^i x^{i-\frac{1}{2}}}{i! 2^{2i+\frac{1}{2}} \Gamma\left(i+\frac{1}{2}\right) \left[N(1-\nu)\right]^{i+\frac{1}{2}}}, \tag{11}$$

where

$$\nu = \frac{1}{m_H m_{h2}} \left[\frac{\Gamma\left(m_H + \frac{1}{2}\right)}{\Gamma\left(m_H\right)}\right]^2 \left[\frac{\Gamma\left(m_{h2} + \frac{1}{2}\right)}{\Gamma\left(m_{h2}\right)}\right]^2, \tag{12}$$

$\lambda = \frac{N\nu}{1-\nu}$, and $\gamma(.,.)$ is the lower incomplete gamma function.

We continue to introduce the following two Lemmas to evaluate the proposed system performance.

Lemma 1. The closed-form expression of the SCP, i.e., Ω_s, for the considered IRS NOMA MEC system based on the proposed IRS-NOMA scheme under quasi-static Nakagami-m fading is as follows:

$$\Omega_s = e^{-\frac{\gamma_1^{th}}{\rho\eta\gamma_U}-\frac{\lambda}{2}} \sum_{i=0}^{\infty} \frac{\lambda^i \Gamma\left(i+\frac{1}{2}, \frac{\gamma_1^{th}\gamma_2^{th}}{\rho\eta\gamma_U} + \frac{\gamma_2^{th}}{2N(1-\nu)(1-\rho)\mu\gamma_U}\right)}{i! 2^{2i+\frac{1}{2}} \Gamma\left(i+\frac{1}{2}\right) \left[\frac{N(1-\nu)(1-\rho)\mu\gamma_1^{th}}{\rho\eta} + \frac{1}{2}\right]^{i+\frac{1}{2}}}, \tag{13}$$

where $\gamma_1^{th} = 2^{\frac{L_1}{BT'}} - 1$, $\gamma_2^{th} = 2^{\frac{L_2}{BT'}} - 1$, $T' = T - \frac{\xi(L_1+L_2)}{f}$, and $\Gamma(.,.)$ is the upper incomplete gamma function.

Proof. Expanding definition (5) with formulas (6), (7), we have:

$$\begin{aligned}
\Omega_s &= \Pr\left(\tau_1 + \tau_2 \le T\right) \\
&= \Pr\left(\max\left\{\frac{L_1}{B\log_2(1+\gamma_{U_1})}, \frac{L_2}{B\log_2(1+\gamma_{U_2})}\right\} + \frac{\xi(L_1+L_2)}{f} \le T\right) \\
&= \Pr\left(\gamma_{U_1} > 2^{\frac{L_1}{BT'}} - 1, \gamma_{U_2} > 2^{\frac{L_2}{BT'}} - 1\right) \\
&= \Pr\left(\frac{\rho\gamma_U\eta X}{(1-\rho)\gamma_U\mu Y + 1} > \gamma_1^{th}, (1-\rho)\gamma_U\mu Y > \gamma_2^{th}\right) \\
&= \Pr\left(X > \frac{\gamma_1^{th}\left[(1-\rho)\gamma_U\mu Y + 1\right]}{\rho\gamma_U\eta}, Y > \frac{\gamma_2^{th}}{(1-\rho)\gamma_U\mu}\right) \\
&= \int_a^{\infty} \left\{1 - F_X\left(\frac{\gamma_1^{th}\left[(1-\rho)\gamma_U\mu t + 1\right]}{\rho\gamma_U\eta}\right)\right\} f_Y(t)dt \\
&\overset{(1)}{=} \int_a^{\infty} e^{-\frac{\gamma_1^{th}\left[(1-\rho)\gamma_U\mu t+1\right]}{\rho\gamma_U\eta}} e^{-\frac{t}{2N(1-\nu)}-\frac{\lambda}{2}} \sum_{i=0}^{\infty} \frac{\lambda^i t^{i-\frac{1}{2}}}{i! 2^{2i+\frac{1}{2}} \Gamma\left(i+\frac{1}{2}\right) \left[N(1-\nu)\right]^{i+\frac{1}{2}}} dt \\
&= e^{-\frac{\gamma_1^{th}}{\rho\gamma_U\eta}-\frac{\lambda}{2}} \sum_{i=0}^{\infty} \frac{\lambda^i}{i! 2^{2i+\frac{1}{2}} \Gamma\left(i+\frac{1}{2}\right) \left[N(1-\nu)\right]^{i+\frac{1}{2}}} \int_a^{\infty} e^{-\left[\frac{(1-\rho)\mu\gamma_1^{th}}{\rho\eta} + \frac{1}{2N(1-\nu)}\right]t} t^{i-\frac{1}{2}} dt \\
&\overset{(2)}{=} e^{-\frac{\gamma_1^{th}}{\rho\gamma_U\eta}-\frac{\lambda}{2}} \sum_{i=0}^{\infty} \frac{\lambda^i \Gamma\left(i+\frac{1}{2}, \frac{(1-\rho)\mu\gamma_1^{th}a}{\rho\eta} + \frac{a}{2N(1-\nu)}\right)}{i! 2^{2i+\frac{1}{2}} \Gamma\left(i+\frac{1}{2}\right) \left[\frac{N(1-\nu)(1-\rho)\mu\gamma_1^{th}}{\rho\eta} + \frac{1}{2}\right]^{i+\frac{1}{2}}}.
\end{aligned}$$

where $T' = T - \frac{\xi(L_1+L_2)}{f}$, $\gamma_1^{th} = 2^{\frac{L_1}{BT'}} - 1$, $\gamma_2^{th} = 2^{\frac{L_2}{BT'}} - 1$, $a = \frac{\gamma_2^{th}}{(1-\rho)\mu\gamma_U}$, step (1) is obtained by substituting $F_X(x) = 1 - e^{-x}$ and (11), step (2) is obtained by applying the result of Eq. (3.381–3) in [31]. This concludes our proof.

Lemma 2. The SCP, i.e., Ω_s, for the considered IRS NOMA MEC system based on the proposed IRS-NOMA scheme under quasi-static Nakagami-m fading when operating in a high transmit SNR regime, approaches the ceiling as follows:

$$\Omega_s^{\infty} = e^{-\frac{\lambda}{2}} \sum_{i=0}^{\infty} \frac{\lambda^i}{i! 2^{2i+\frac{1}{2}} \left[\frac{N(1-\nu)(1-\rho)\mu\gamma_1^{th}}{\rho\eta} + \frac{1}{2}\right]^{i+\frac{1}{2}}}. \tag{14}$$

Proof. When $\gamma_U \to \infty$, $\lim_{\gamma_U \to \infty} e^{-\frac{\gamma_1^{th}}{\rho\eta\gamma_U}} \to 1$ and $\lim_{\gamma_U \to \infty} \Gamma\left(i + \frac{1}{2}, \frac{\gamma_1^{th}\gamma_2^{th}}{\rho\eta\gamma_U} + \frac{\gamma_2^{th}}{2(1-\rho)b\gamma_U}\right) \to \Gamma\left(i + \frac{1}{2}\right)$. Thus, the upper bound of Ω_s can be obtained as (14). This concludes our proof.

4 Numerical Results and Discussion

In this section, we provide the numerical results and discussions of SCP-based system performance. Table 1 summarizes the Monte-Carlo simulation parameters to be used in the next part of this manuscript [21].

Table 1. Simulation parameters

Parameters	Notation	Typical values
Environment		Nakagami-m
Nakagami fading parameters	m_H, m_{h2}	3, 1.5
Distances	d_1, d_{21}, d_{22}	10 m, 40 m, 10 m
Path-loss exponents	α_1, α_2	3.5, 2.5
Number of IRS' elements	N	18, 24, 30
The transmit power	P_U	10–40 dB
The CPU-cycle frequency of MEC server	f	1 GHz
The number of CPU cycles of MEC server for executing each bit	ρ	5
The channel bandwidth	B	300–800 MHz
The threshold of latency	T	1 s
The total data bits of user tasks	L	0.5–1.5 Mbits
The length of U_1's task	L_1	0.4 L Mbits
The length of U_2's task	L_2	0.6 L Mbits

4.1 The Impact of the Average Transmit SNR and the Number of IRS Elements

Figure 3 depicts the curves of successful computation probability Ω_s been subject to the average transmit SNR (γ_U) and the different number of IRS elements (N). When the γ_U increase, Ω_s increases. When γ_U rises too high above 35 dB, Ω_s gradually approaches saturation value. Another observation in Fig. 3 is that when N increases, Ω_s increases. It is consistent with the fact that when the number

of IRS elements increases, it means U_2 will be better supported for offloading, leading to improved performance of the whole system.

However, the effects of N on SCP are clearly observable only in cases where γ_U has a low value. In the opposite case, as observed in the accompanying small figure, increasing N can improve Ω_s very little, only about 0.1 %. To put it more simply, the IRS NOMA MEC system can be designed with a low number of IRS elements when the transmitting power of the devices is large enough.

The key fact to remember is that the SCP can be improved by increasing the transmit power and/or the number of IRS elements.

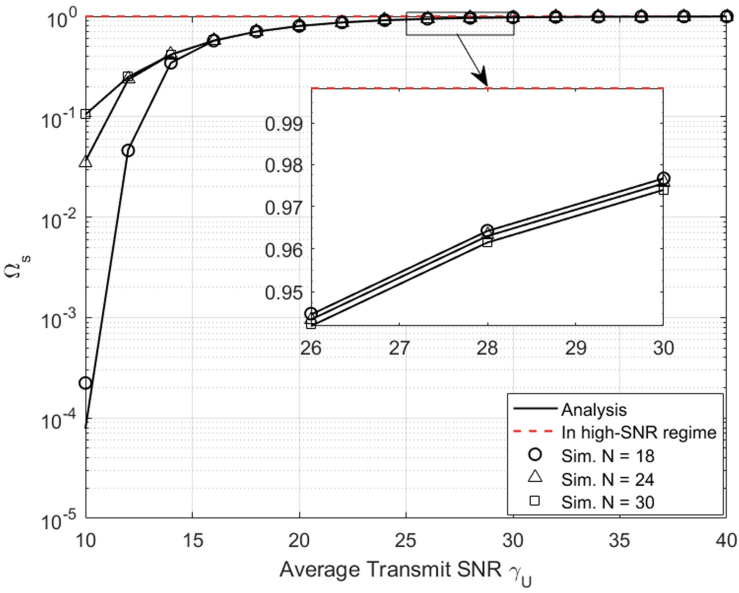

Fig. 3. Ω_s vs. average transmit SNR γ_U with different N.

4.2 The Impact of the Task Length and the Bandwidth

In this experiments, we investigate the impact of the task length (L) and the bandwidth (B) on Ω_s, which are depicted as Fig. 4 and Fig. 5, respectively. We can observe that Ω_s increases when L decreases. It is consistent with the formulas (6) and (7), when L decreases, the time to offload and calculate the tasks decreases, leading to the probability that the tasks are completed within the time T allows increase. However, the effect of L on Ω_s is only clearly observed when (γ_U) is low.

The result from Fig. 5 shows that when we increase the bandwidth, system performance is improved. The formula (6) could explain this result: As B increases, τ_1 decreases, meaning less time is needed to offload tasks, leading to improved Ω_s. We conclude that the SCP of proposed system can be improved by increasing the bandwidth and/or decreasing the task length.

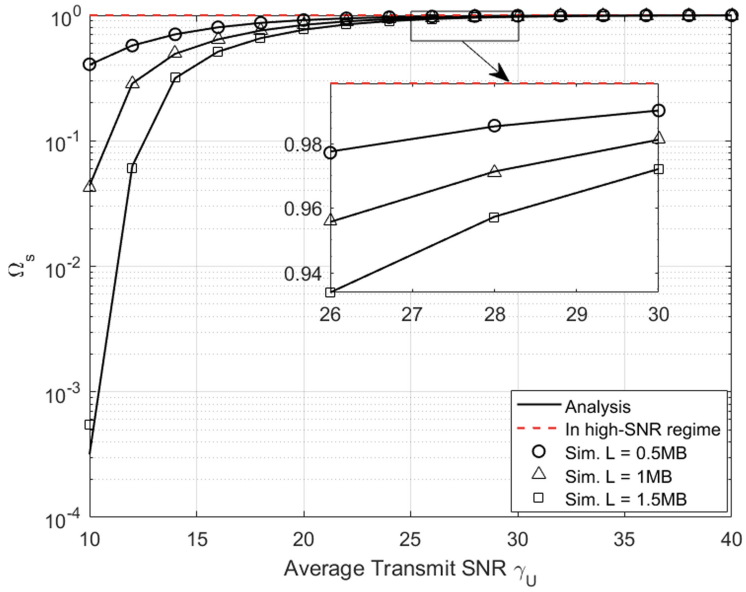

Fig. 4. Ω_s vs. average transmit SNR γ_U with different task length L.

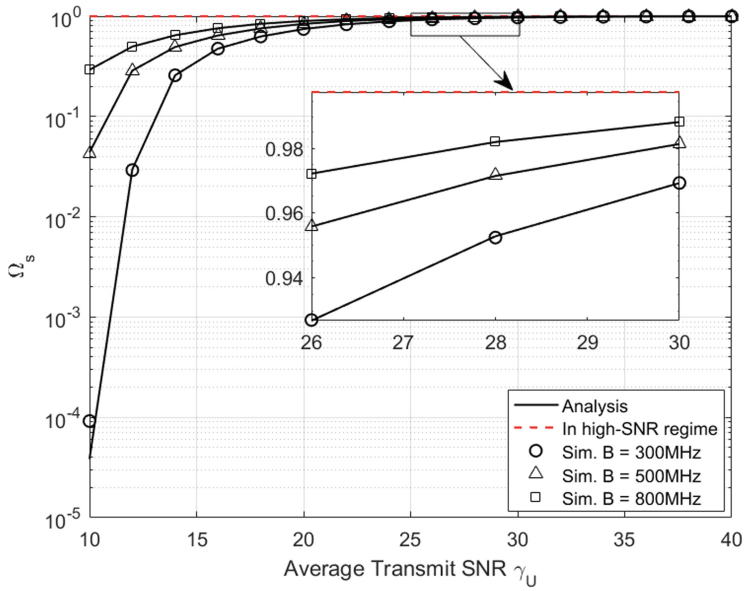

Fig. 5. Ω_s vs. average transmit SNR γ_U with different bandwidth B.

4.3 The Impact of Power Allocation Coefficient

The curves in Fig. 6 demonstrate the impact of power allocation coefficient (ρ) on Ω_s with different transmit power levels. Again, this figure shows that the system's SCP responds as γ_0 increases.

According to the form of three SCP curves, we state that Ω_s increases when ρ increases from 0 to ρ^*. In contrary Ω_s falls when ρ increases from ρ^* to 1, where ρ^* is the optimal value for maximization of Ω_s.

From Fig. 3, 4 and 5, when $\gamma_U \to \infty$ the ceiling of Ω_s is nearly 1. It means that in a high-SNR regime, Ω_s approaches 1. Referring to the views of the above results, we can state that the agreement between simulation and analysis results is good, confirming our analysis's accuracy.

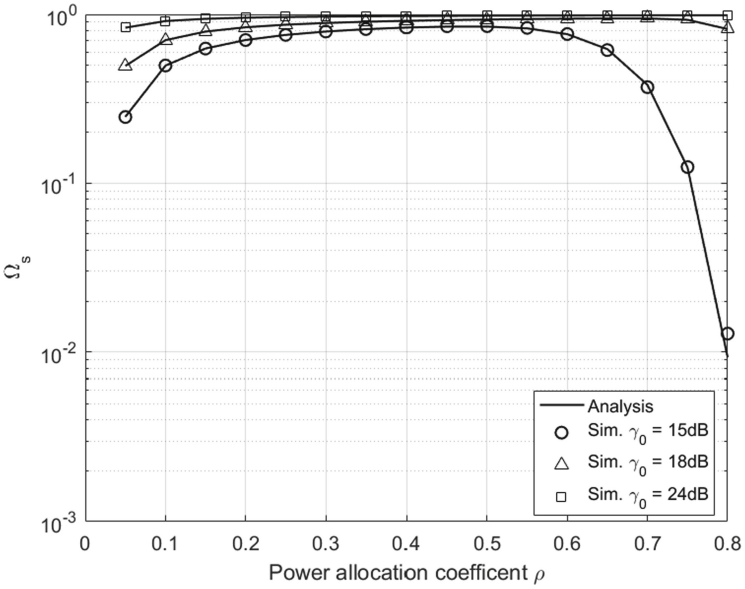

Fig. 6. Ω_s vs. power allocation coefficient ρ with different γ_U.

5 Conclusion

In this paper, we have studied the performance of an IRS-assisted NOMA MEC system. Accordingly, we propose a 4-phase IRS-NOMA protocol for the system, including the parameter determining, offloading, computing, and result returning phases. We derive the closed-form expressions of successful computation probability and its ceiling in the high-SNR regime. Furthermore, the impacts of critical system parameters, such as the transmit SNR, the number of IRS elements, the task length, bandwidth, and the power allocation coefficient on the behavior of this considered system, have been evaluated to look insight into the performance.

In order to improve the system performance, we can increase the transmit SNR, number of IRS elements, and bandwidth or decrease the task length or select the optimal power allocation coefficient. We will focus on the multiple users wireless power transfer of this IRS NOMA MEC system in future work.

References

1. Pham, Q.V., Fang, F., Ha, V.N., Piran, M.J., Le, M., Le, L.B., Hwang, W.J., et al.: A survey of multi-access Edge Computing in 5G and beyond: fundamentals, technology integration, and state-of-the-art. IEEE Access **8**, 116974–117017 (2020)
2. Mao, Y., You, C., Zhang, J., Huang, K., Letaief, K.B.: A survey on mobile edge computing: the communication perspective. IEEE Commun. Surv. Tutor. **19**(4), 2322–2358 (2017)
3. Zhou, F., Wu, Y., Hu, R.Q., Qian, Y.: Computation efficiency in a wireless-powered mobile edge computing network with NOMA. In: IEEE International Conference on Communications (ICC), 20–24 May 2019, Shanghai, China (2019)
4. Ding, Z., Fan, P., Poor, H.V.: Impact of non-orthogonal multiple access on the offloading of mobile edge computing. IEEE Trans. Commun. **67**(1), 375–390 (2019)
5. Wang, F., Xu, J., Ding, Z.: Multi-antenna noma for computation offloading in multiuser mobile edge computing systems. IEEE Trans. Commun. **67**(3), 2450–2463 (2019)
6. Truong, V.T., Ha, D.B., So-In, C., et al.: On the system performance of mobile edge computing in an uplink NOMA WSN with a multiantenna access point over nakagami-m fading. IEEE/CAA J. Automatica Sinica **9**(4), 668–685 (2022)
7. Akbar, A., Sobia Jangsher, F.A.B.: NOMA and 5G emerging technologies: a survey on issues and solution techniques. Comput. Netw. **190**, 107950 (2021). https://doi.org/10.1016/j.comnet.2021.107950
8. Maraqa, O., Rajasekaran, A.S., Al-Ahmadi, S., Yanikomeroglu, H., Sait, S.M.: A survey of rate-optimal power domain NOMA with enabling technologies of future wireless networks. IEEE Commun. Surv. Tut. **22**(4), 2192–2235, 107950 (2020)
9. Duong, T.Q., Bao, V.N.Q.: Performance analysis of selection decode-and-forward relay networks. Electron. Lett. **44**(20), 1206–1207 (2008)
10. Fan, L., Zhang, S., Duong, T.Q., Karagiannidis, G.K.: Secure switch-and-stay combining (SSSC) for cognitive relay networks. IEEE Trans. Commun. **64**(1), 70–82, 107950 (2015)
11. Truong, V.T., Vo, M.T., Lee, Y., Ha, D.B.: Amplify-and-forward relay transmission in uplink non-orthogonal multiple access networks. In: 2019 6th NAFOSTED Conference on Information and Computer Science (NICS), pp. 1–6 (2019). https://doi.org/10.1109/NICS48868.2019.9023818
12. Li, D., Li, B., Qin, N., Jing, X., Du, C., Wan, C.: The research of NOMA-MEC network based on untrusted relay-assisted transmission in power internet of things. IOP Conf. Ser. Earth Environ. Sci. **634**, 012052 (2021)
13. Di Renzo, M., et al.: Reconfigurable intelligent surfaces vs. relaying: differences, similarities, and performance comparison. IEEE Open J. Commun. Soc. **1**, 798–807, 012052 (2020)
14. Alghamdi, R.: Intelligent surfaces for 6G wireless networks: a survey of optimization and performance analysis techniques. IEEE Access **8**, 202795–202818, 012052 (2020). https://doi.org/10.1109/ACCESS.2020.3031959

15. Dai, L.: Reconfigurable intelligent surface-based wireless communications: antenna design, prototyping, and experimental results. IEEE Access **8**, 45913–45923, 012052 (2020). https://doi.org/10.1109/ACCESS.2020.2977772
16. Chen, Z., Ma, X., Han, C., Wen, Q.: Towards intelligent reflecting surface empowered 6g terahertz communications: a survey. China Commun. **18**(5), 93–119 (2021). https://doi.org/10.23919/JCC.2021.05.007
17. Bai, T., Pan, C., Deng, Y., Elkashlan, M., Nallanathan, A., Hanzo, L.: Latency minimization for intelligent reflecting surface aided mobile edge computing. IEEE J. Sel. Areas Commun. **38**, 2666–2682 (2020)
18. Chu, Z., Xiao, P., Shojafar, M., Mi, D., Mao, J., Hao, W.: Intelligent reflecting surface assisted mobile edge computing for internet of things. IEEE Wireless Commun. Lett. **10**(3), 619–623, 012052 (2021). https://doi.org/10.1109/LWC.2020.3040607
19. Yang, G., Xu, X., Liang, Y.: Intelligent reflecting surface assisted non-orthogonal multiple access. In: 2020 IEEE Wireless Communications and Networking Conference (WCNC), pp. 1–6 (2020). https://doi.org/10.1109/WCNC45663.2020.9120476
20. Zheng, B., Wu, Q., Zhang, R.: Intelligent reflecting surface-assisted multiple access with user pairing: NOMA or OMA? IEEE Commun. Lett. **24**(4), 753–757 (2020). https://doi.org/10.1109/LCOMM.2020.2969870
21. Cheng, Y., Li, K.H., Liu, Y., Teh, K.C., Vincent Poor, H.: Downlink and uplink intelligent reflecting surface aided networks: NOMA and OMA. IEEE Trans. Wireless Commun. **20**(6) (2021). https://doi.org/10.1109/twc.2021.3054841
22. Zhou, F., You, C., Zhang, R.: Delay-optimal scheduling for IRS-aided mobile edge computing. IEEE Wireless Commun. Lett. **10**, 740–744 (2021). https://doi.org/10.1109/LWC.2020.3042189
23. Chen, G., Wu, Q., Chen, W., Ng, D.W.K., Hanzo, L.: IRS-aided wireless powered MEC systems: TDMA or NOMA for computation offloading? 2108.06120 (2021)
24. Wang, Q., Zhou, F., Hu, H., Hu, R.Q.: Energy-efficient design for IRS-assisted MEC networks with NOMA. In: 2021 13th International Conference on Wireless Communications and Signal Processing (WCSP) (IEEE), pp. 1–6 (2021)
25. Li, X., Xie, Z., Chu, Z., Menon, V.G., Mumtaz, S., Zhang, J.: Exploiting benefits of IRS in wireless powered NOMA networks. IEEE Trans. on Green Commun. Netw. **6**(1), 175–186 (2022). https://doi.org/10.1109/TGCN.2022.3144744
26. Okogbaa, F.C., et al.: Design and application of intelligent reflecting surface (IRS) for beyond 5G wireless networks: a review. Sensors **22**(7), 2436 (2022)
27. Chu, Z., Xiao, P., Shojafar, M., Mi, D., Mao, J., Hao, W.: Intelligent reflecting surface assisted Mobile Edge Computing for Internet of Things. IEEE Wireless Commun. Lett. **10**(3), 619–623 (2020)
28. Truong, V.T., Ha, D.B., Lee, Y., Nguyen, A.N.: On performance of cooperative transmission in Uplink Non-orthogonal Multiple Access wireless sensor networks. In: Proceedings of the 4th International Conference on Recent Advance in Signal Processing, Telecommunications and Computing (SigTelCom) (IEEE), pp. 56–60 (2020)
29. Ye, Y., Lu, G., Hu, R.Q., Shi, L.: On the performance and optimization for MEC networks using uplink NOMA. In: IEEE International Conference on Communications Workshops (ICC Workshops), Shanghai, China (IEEE) (2019)

30. Nguyen, A.N., So-In, C., Ha, D.B., Truong, V.T. et al.: Performance analysis in UAV-enabled relay with NOMA under Nakagami-m fading considering adaptive power splitting. In: 2021 18th International Joint Conference on Computer Science and Software Engineering (JCSSE) (IEEE), pp. 1–6 (2021)
31. Gradshteyn, I., Ryzhik, I.: Table of Integrals, Series, and Products. Elsevier Academic Press (2007)